

Cerebral blood flow predicts multiple demand network activity and fluid intelligence across the lifespan

SHUYI WU^{1,2}, LORRAINE K. TYLER¹, RICHARD N.A. HENSON³, JAMES B. ROWE^{3,4}, CAM-CAN^{1,4}, KAMEN A. TSVETANOV^{1,4,*}

* Corresponding author (kat35@cam.ac.uk, +44 1223 766 556)

¹ Centre for Speech, Language and the Brain, Department of Psychology, University of Cambridge, Cambridge, UK

² Department of Management, School of Business, Hong Kong Baptist University, Hong Kong, China

³ Medical Research Council Cognition and Brain Sciences Unit, Department of Psychiatry, Cambridge, UK

⁴ Department of Clinical Neurosciences, University of Cambridge, Cambridge, UK

Abstract:

The preservation of cognitive function into old age is a public health priority. Cerebral hypoperfusion is a hallmark of dementia but its impact on maintaining cognitive ability across the lifespan is less clear. We investigated the relationship between baseline cerebral blood flow (CBF) and blood oxygenation level-dependent (BOLD) response during a fluid reasoning task in a population-based adult lifespan cohort (N=227, age 18-88 years). As age differences in baseline CBF could lead to non-neuronal contributions to the BOLD signal, we introduced commonality analysis to neuroimaging, in order to dissociate performance-related CBF effects from the physiological confounding effects of CBF on the BOLD response. Accounting for CBF, we confirmed that performance- and age-related differences in BOLD responses in the multiple-demand network (MDN) implicated in fluid reasoning. Differences in baseline CBF across the lifespan explained not only performance-related BOLD responses, but also performance-independent BOLD responses. Our results suggest that baseline CBF is important for maintaining cognitive function, while its non-neuronal contributions to BOLD signals reflect an age-related confound. Maintaining perfusion into old age may serve to support brain function with behavioural advantage, regulating brain health.

Keywords (up to five): ageing, functional magnetic resonance imaging (fMRI), cerebral blood flow, multiple demand network, commonality analysis

1 1. Introduction

2

3 The world's population is ageing, with every sixth person expected to be over 65 by 2050
4 (United Nations, 2020). Cognitive decline has emerged as a major health threat in old age,
5 including but not limited to dementia (Piguet et al., 2009; Yarchoan et al., 2012). To combat this
6 threat, there is increasing demand to identify factors that facilitate the maintenance of cognitive
7 function across the lifespan. Ageing causes changes to our brains in vascular, structural and
8 functional domains (Kennedy and Raz, 2015; Cabeza et al., 2018). However, these effects are
9 normally reported separately, and only through their integration one can better understand how
10 these domains influence cognitive decline in old age (Tsvetanov et al., 2021).

11 Cerebral blood flow (CBF) changes early in experimental models of dementia, leading to
12 neuronal dysfunction, and loss independently of amyloid- β -dependent contributions (Iadecola,
13 2004; Zlokovic, 2011; Kisler et al., 2017; Sweeney et al., 2018, 2019). In healthy ageing, previous
14 reports have linked the effects of age on baseline CBF to behavioural performance measured
15 outside of the scanner (Bangen et al., 2014; Hays et al., 2017; Leeuwis et al., 2018). However,
16 brain perfusion measurements are highly dependent on other physiological factors such as
17 autoregulation modulators (Lemkuil et al., 2013), medication, time of day, levels of wakefulness
18 (Patricia et al., 2014), physical exercise, caffeine or smoking before the scan (Domino et al., 2004;
19 Addicott et al., 2009; Merola et al., 2017). Therefore, differences in CBF signal may reflect an age-
20 related bias in such factors, rather than a true baseline difference in CBF (Grade et al., 2015).
21 Moreover, it remains unclear whether the observed CBF dysregulation in ageing reflects a link
22 between somatic differences in vascular health and global cognition, or whether CBF modifies
23 regional brain activations underlying specific cognitive processes. To understand the role of
24 baseline CBF in cognitive ageing, one must also test whether baseline CBF is associated with
25 performance-related brain activity during cognitive tasks.

26 The field of neurocognitive ageing research has often used functional magnetic resonance
27 imaging (fMRI) to study age differences in brain activity during cognitive tasks. fMRI data are
28 usually interpreted in terms of neuronal activity, but the blood oxygenation level-dependent
29 (BOLD) signal measured by fMRI also reflect vascular differences and neurovascular coupling
30 (Mishra et al., 2021), which changes with age (Tsvetanov et al., 2021). Failure to account for
31 vascular health alterations leads to misinterpretation of fMRI BOLD signals (Hutchison et al.,
32 2013; Liu et al., 2013; Tsvetanov et al., 2015) and their cognitive relevance (Geerligs and
33 Tsvetanov, 2016; Tsvetanov et al., 2016; Geerligs et al., 2017). Several approaches exist to
34 separate vascular from neural contributions to the BOLD signals, including the use of baseline
35 CBF to normalise for age differences in cerebrovascular function (Tsvetanov et al., 2021).
36 Normalisation with baseline CBF would improve detection of "true" neuronal changes i.e., over
37 and above age-related differences in non-neuronal physiology. This would control for
38 behaviourally irrelevant *confounding effects*, and *performance-related effects* where cerebral
39 hypoperfusion reflects neuronal function and loss. Therefore, it would be better to integrate,
40 not simply control for, baseline CBF differences in task-based BOLD studies to dissociate
41 confounding from performance-related effects of CBF on age-related differences in the BOLD
42 fMRI responses.

43 To distinguish confounding from performance effects of CBF is important to understand
44 the neuronal substrates of multiple cognitive demands with ageing (Kaufman and Horn, 1996;
45 Salthouse, 2012; Kievit et al., 2014). Demanding, complex or executive functions depend on a
46 distributed network of brain regions known as the multiple-demand network (MDN), which is
47 readily activated during tasks used to assess fluid intelligence (Crittenden et al., 2016;
48 Tschentscher et al., 2017; Woolgar et al., 2018). The MDN parses complex tasks into
49 subcomponents or sub-goals (Duncan, 2013; Camilleri et al., 2018). There is substantial spatial
50 overlap between MDN and the brain regions with impaired baseline CBF in ageing (Tsvetanov et
51 al., 2020b, 2021). Therefore, some of the age differences in MDN and cognition (Tsvetanov et al.,
52 2016; Samu et al., 2017) may reflect confounding and/or performance-related effects of CBF
53 dysregulation.

54 To characterise neurocognitive ageing, we propose the use of commonality analysis to
55 dissociate *confounding* from *performance-related* effects of CBF on age-related differences in
56 brain functional measures. Commonality analysis, unlike the normalisation approach, allows for
57 adjustment of multiple variables simultaneously by identifying the variance in a dependent
58 variable associated with each predictor uniquely, as well as the variance in common to two or
59 more predictors (Nimon et al., 2008; Kraha et al., 2012). Here, we identify unique and common
60 effects of age, performance, and baseline CBF on fMRI BOLD responses during a fluid reasoning
61 task in a population-based adult lifespan cohort (age 18-88, N = 227, www.camcan.org).
62 Reasoning was measured by the common Cattell task of fluid intelligence, which requires solving
63 a number of problems, and is known to decline dramatically with age (Kievit et al., 2014).

64 We predicted that the integration of baseline CBF with task-based fMRI BOLD would
65 improve detection of confounding and performance-related effects of CBF associated with
66 reasoning. Performance-related effects of CBF would be indicated by variance in the BOLD
67 response that is common to age, task performance and CBF, whereas confounding effects of CBF
68 would be indicated by variance that is common to age and CBF, but not shared with performance.

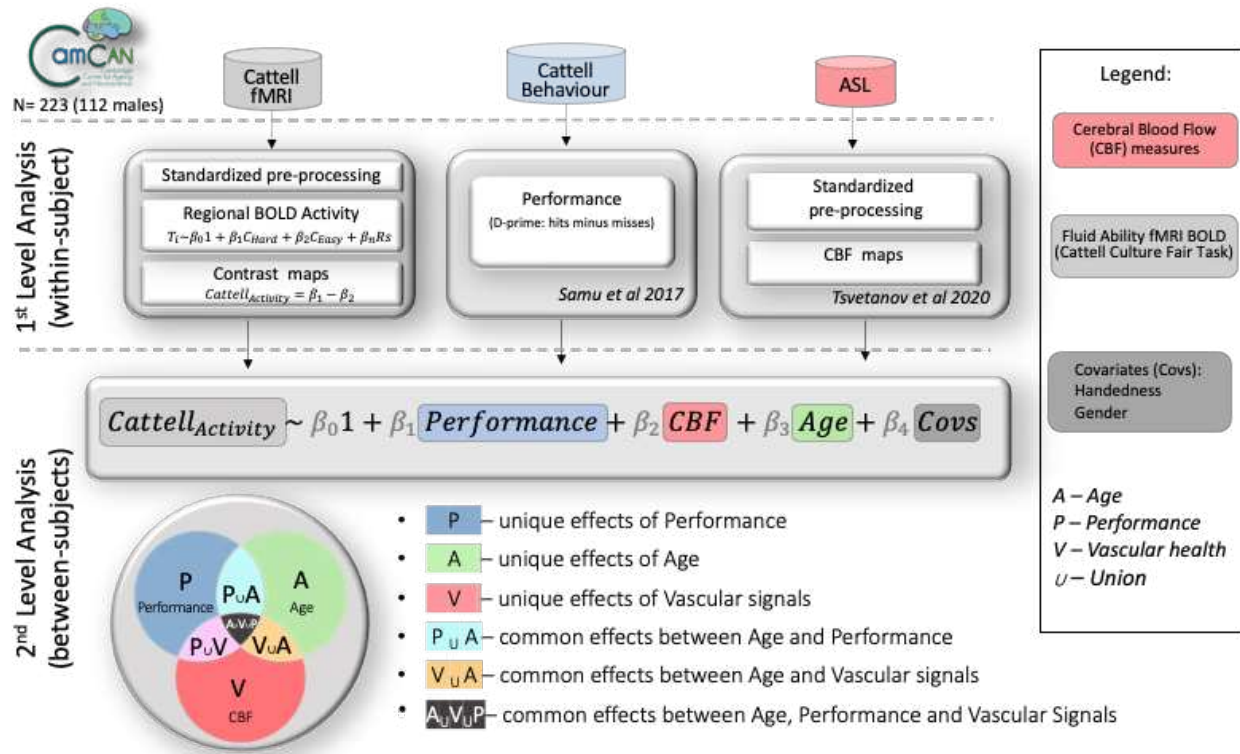
69 2. Methods

70 2.1. Participants

71 Figure 1 illustrates the study design, data processing and analysis pipeline. The data were
72 acquired from Phase 3 of the Cambridge Centre for Aging and Neuroscience (Cam-CAN), a large
73 population-based study of the healthy adult life span (Shafto et al., 2014; Taylor et al., 2015). The
74 ethical approval for the study was approved by the Cambridge 2 Research Ethics Committee and
75 written informed consent was provided by all participants. Exclusion criteria included poor
76 hearing (a sensitive threshold of 35 dB at 1000 Hz in both ears) and poor vision (below 20/50 on
77 the Snellen test; Snellen, 1862), low Mini-Mental Status Examination (Folstein et al., 1975), self-
78 reported substance abuse as assessed by the Drug Abuse Screening Test (Skinner, 1982),
79 significant psychiatric disorders (e.g., schizophrenia, bipolar disorder, personality disorder), or
80 neurological diseases (e.g. a history of stroke, epilepsy, traumatic brain injury). Demographic
81 characteristics of the sample are described in Table 1.

82

83



84
85

Figure 1. Summary of the analytical pipeline.

86
87

2.2. Stimuli, task and procedure

Participants undertook a Fluid Intelligence task which draws on critical cognitive processes of fluid reasoning, which underlies many complex cognitive operations (Duncan, 2013), and which declines with age (Horn and Cattell, 1967; Kaufman and Horn, 1996; Salthouse et al., 2003; Duncan, 2010; Salthouse, 2012; Kievit et al., 2014). We used a simplified version of the Cattell Culture Fair test (Cattell, 1971), modified to be used in the scanner (Woolgar et al., 2013; Samu et al., 2017). On each trial, participants were presented with a display of four patterns and had to select the “odd one out”. The task employed a block design, with 30-seconds blocks of trials alternating between two conditions with different difficulty level (“easy” and “hard” puzzles). There was a total of four blocks per condition. Because there was a fixed time to perform as many trials as possible, behavioural performance was measured by subtracting the number of incorrect trials from the number of correct trials (averaged over hard and easy blocks, following Samu et al., (2017), i.e. to ensure that someone responding quickly but randomly did not score highly. The suitability of this performance score was confirmed by its strong correlation (Pearson’s $r[95\% \text{ CI}]$): $r(223) = 0.70 [0.63, 0.76]$, $P < 0.001$) with scores obtained from the full version of the Cattell test, administered outside the scanner at stage 2 of Cam-CAN (Shafto et al., 2014). We also excluded $n = 28$ participants who had disproportionately poor performance with 10 or more incorrect trials

105 (17 females, with age range 31-88); leaving N = 223 remaining (111 females, age range 19 - 87
106 years).

107

108 2.3. MRI Acquisition and Preprocessing

109 Imaging data were acquired using a 3T Siemens TIM Trio System with a 32-channel head-
110 coil at the MRC Cognition and Brain sciences Unit (CBU; www.mrc-cbu.cam.ac.uk). Of the initial
111 cohort, 256 participants had valid T1, T2, arterial spinning labelling (ASL) data, and task-induced
112 BOLD data from a fluid intelligence task.

113 A 3D-structural MRI was acquired on each participant using T1-weighted sequence
114 (Generalized Auto-calibrating Partially Parallel Acquisition (GRAPPA) with the following
115 parameters: repetition time (TR) = 2,250 ms; echo time (TE) = 2.99 ms; inversion time (TI) = 900
116 ms; flip angle α = 9°; field of view (FOV) = $256 \times 240 \times 192 \text{ mm}^3$; resolution = 1 mm isotropic;
117 accelerated factor = 2; acquisition time, 4 min and 32 s.

118 We used Release003 of the CamCAN Automatic Analysis pipelines for Phase III data
119 (Taylor et al.,(2015), which called functions from SPM12 (Wellcome Department of Imaging
120 Neuroscience, London, UK). The T1 image from Phase II was rigid-body coregistered to the MNI
121 template, and the T2 image from Phase II was then rigid-body coregistered to the T1 image. The
122 coregistered T1 and T2 images were used in a multimodal segmentation to extract probabilistic
123 maps of six tissue classes: gray matter (GM), white matter (WM), CSF, bone, soft tissue, and
124 residual noise. The native space GM and WM images were submitted to diffeomorphic
125 registration to create group template images. Each template was normalized to the MNI
126 template using a 12-parameter affine transformation.

127

128 2.4. EPI image acquisition and processing

129 For the Cattell-based fMRI in Phase III of CamCAN, Gradient-Echo-Planar Imaging
130 (EPI) of 150 volumes captured 32 axial slices (sequential descending order) of thickness of 3.7
131 mm with a slice gap of 20% for whole-brain coverage with the following parameters: TR = 1970
132 ms; TE = 30 ms; flip angle α = 78°; FOV = $192 \times 192 \text{ mm}^2$; resolution = $3 \times 3 \times 4.44 \text{ mm}^3$, with
133 a total duration of 5 min.

134 EPI data preprocessing included the following steps: (1) spatial realignment to adjust for
135 linear head motion, (2) temporal realignment of slices to the middle slice, (3) coregistration to
136 the T1 anatomical image from Phase II above, (4) application of the normalization parameters
137 from the T1 stream above to warp the functional images into MNI space, and (5) smoothing by
138 an 8mm Gaussian kernel.

139 For the participant-level modelling, every voxel's time-course was regressed in a multiple
140 linear regression on the task's design matrix which consisted of time-courses for hard and easy
141 conditions convolved with a canonical haemodynamic response function (HRF). Regressors of no
142 interest included WM, CSF, 6 standard realignment parameters (accounting for in-scanner head
143 motions), and harmonic regressors that capture low-frequency changes (1/128 Hz) in the signal
144 typically associated with scanner drift and physiological noise. WM and CSF signals were
145 estimated for each volume from the mean value of WM and CSF masks derived by thresholding
146 SPM's tissue probability maps at 0.75. The contrast of parameter estimates for hard minus easy
147 conditions for each voxel and participant was then calculated, termed here *Cattell activation*.

148

149 2.5. Arterial spinning labelling (ASL) image acquisition and processing

150 Perfusion-weighted images of cerebral blood flow used pulsed arterial spin labelling
151 (PASL, PICORE-Q2T-PASL with background suppression). The sequence is used with the following
152 parameters: repetition time (TR) = 2500 ms, echo time (TE) = 13 ms, field of view (FOV) = 256 ×
153 256 × 100 mm³, 10 slices, 8 mm slice thickness, flip angle = 90°, inversion time 1 (TI1) = 700 ms,
154 TI2 = 1800 ms, Saturation stop time = 1600 ms, tag width = 100 mm and gap = 20.9 mm, 90
155 repetitions giving 45 control-tag pairs, voxel-size = 4 mm × 4 mm × 8 mm, 25% interslice gap,
156 acquisition time of 3 minutes and 52 seconds. In addition, a single-shot EPI (M0) equilibrium
157 magnetization scan was acquired. Pulsed arterial spin labelling time series were converted to
158 maps of CBF using Explore ASL toolbox (<https://github.com/ExploreASL/ExploreASL>; Mutsaerts
159 et al., 2018). Following rigid-body alignment, the images were coregistered with the T1 from
160 Phase II above, normalised with normalization parameters from the T1 stream above to warp ASL
161 images into MNI space and smoothed with a 12 mm FWHM Gaussian kernel (for more details,
162 Tsvetanov et al., 2020b).

163

164 2.6. Analytical approach

165

166 To model random effects across participants, we performed voxel-wise analysis using
167 multiple linear regression (MLR) with age as the main independent variable of interest, and sex
168 and handedness as covariates of no interest. This MLR was applied to maps of both Cattell
169 activation (BOLD) and baseline CBF.

170 To evaluate the confounding and performance-related effects of resting CBF on BOLD
171 activation, we conducted commonality analysis (Nimon et al., 2008; Kraha et al., 2012).
172 Commonality analysis partitions the variance explained by all predictors in MLR into variance
173 unique to each predictor and variance shared between each combination of predictors.
174 Therefore, unique effects indicate the (orthogonal) variance explained by one predictor over and
175 above that explained by other predictors in the model, while common effects indicate the
176 variance shared between correlated predictors. Notably, the sum of variances, also known as
177 commonality coefficients, equals the total R² for the regression model.

178 We adapted a commonality analysis algorithm (Nimon et al., 2008) for neuroimaging
179 analysis to facilitate voxel-wise nonparametric testing in Matlab (Mathworks,
180 <https://uk.mathworks.com/>). The commonality analysis was applied the Cattell activation in
181 each voxel separately (see Figure 1). The independent variables in the model were baseline CBF
182 for the corresponding voxel, age and task performance. Covariates of no interest included sex
183 and handedness. The model can therefore identify unique variance explained by each of the
184 predictors (U_{CBF}, U_{Age} and U_P for CBF, Age and Performance, respectively). Common effects of
185 interest were the *confounding effects*, defined by the shared variance between CBF and age
186 (C_{CBF, Age}), and *performance-related effects*, defined by the common variance between CBF, Age
187 and Performance (C_{CBF, Age, P}). Significant clusters related to effects of interest were identified
188 with nonparametric testing using 1000 permutations and threshold-free cluster enhancement,
189 corrected to p<.05 (Smith and Nichols, 2009). This Matlab version of commonality analysis for

190 neuroimaging with TFCE implementation is available at
191 <https://github.com/kamentsvetanov/CommonalityAnalysis/>.

192
193
194

195 2.7. Data and code availability

196
197
198
199
200
201
202

The dataset analysed in this study is part of the Cambridge Centre for Ageing and Neuroscience (Cam-CAN) research project (www.cam-can.com). Raw and minimally pre-processed MRI (i.e. from automatic analysis; Taylor et al., 2015) and behavioural data are available by submitting a data request to Cam-CAN (<https://camcan-archive.mrc-cbu.cam.ac.uk/dataaccess/>).

203 Task-based fMRI data was post-processed using SPM12
204 (<http://www.fil.ion.ucl.ac.uk/spm>; Friston et al., 2007). Arterial spin labelling data were post-
205 processed using ExploreASL toolbox (<https://github.com/ExploreASL/ExploreASL>; Mutsaerts et
206 al., 2018). As part of this study, MATLAB-based commonality analysis for neuroimaging with
207 TFCE implementation was developed and made available at
208 <https://github.com/kamentsvetanov/CommonalityAnalysis/>. Visualisation of all neuroimaging
209 results was generated using MRIcroGL (<https://github.com/ordenlab/MRIcroGL>; Rorden and
210 Brett, 2000). The corresponding author (K.A.T.) can provide custom-written analyses code on
211 request.

212

213 3. Results

214 3.1. Main effect and effect of age on BOLD in Cattell task

215 Group-level analysis confirmed activations for the hard vs easy condition in the lateral
216 prefrontal cortex, the anterior insula, the dorsal anterior cingulate cortex, the frontal eye field,
217 the pre-supplementary motor area and areas along the intraparietal sulcus and lateral temporal
218 lobe, recapitulating the multiple demand network (MDN, Duncan, 2013; Camilleri et al., 2018),
219 and the lateral occipital cortex and the calcarine cortex (Figure 2a). Additionally, we observed
220 deactivations in the ventral medial prefrontal cortex (vmPFC), posterior cingulate cortex (PCC)
221 and inferior parietal lobe (IPL), recapitulating the default network (Buckner et al., 2008; Raichle,
222 2015; Buckner and DiNicola, 2019). With respect to ageing, there were weaker activations in
223 regions of the MDN, and weaker deactivations in regions of the DMN, associated with increasing
224 age, see Figure 2b, consistent with previous studies (Samu et al., 2017).

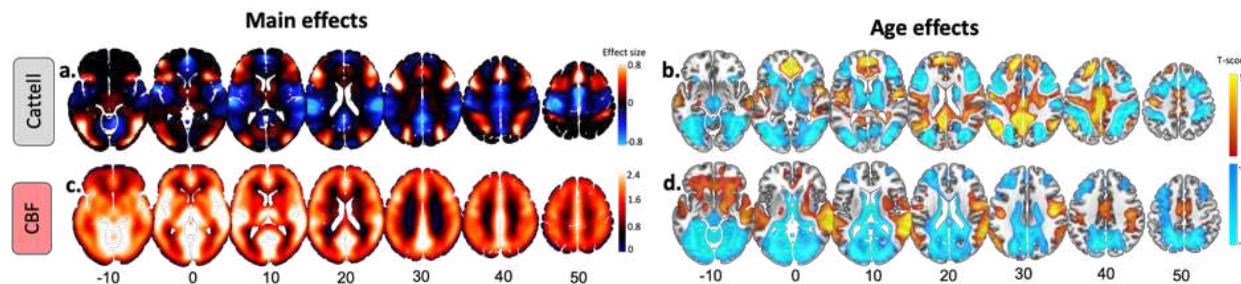
225 3.2. Main effect and effect of age on baseline CBF

226 Group-level results revealed a pattern of relatively high cerebral blood flow in cortical and
227 subcortical brain areas associated with high perfusion and high metabolism (Henriksen et al.,
228 2018; Figure 2c), such as caudal middle-frontal, posterior cingulate, pericalcarine, superior
229 temporal and thalamic regions. Moderate to low CBF values in the superior-parietal and inferior-
230 frontal areas of the cortex (Figure 2c) may reflect the axial positioning of the partial brain
231 coverage sequence used in the study.

232 We observed age-related declines in CBF in the bilateral dorsolateral prefrontal cortex,
233 lateral parietal cortex, anterior and posterior cingulate, pericalcarine, and cerebellum (Figure 2c)
234 in agreement with previous reports (Chen et al., 2011; Zhang et al., 2018). Also, we observed age-
235 related CBF increase in regions susceptible to individual and group differences in arterial transit
236 time that can bias accuracy of CBF estimation, including middle temporal gyrus and middle
237 cingulate cortex (Mutsaerts et al., 2017).

238

239



240

241

242

243

244

245

Figure 2. Main and age effects on task-based activity and cerebral blood flow (CBF) maps. (a) Main effects of BOLD activity in response to Hard vs Easy blocks with over- and under-activations shown in warm and cold colours, respectively. (b) Age-related decreases (cold colours) and increases (warm colours) in Cattell task. (c) Main effect of baseline CBF across all participants. (d) Age-related decreases (cold colours) and increases (warm colours) in baseline CBF. Slices are numbered by z level in Montreal Neurological Institute (MNI) space.

246

3.3. Commonality analysis of BOLD Cattell activation

247

3.3.1. Unique effects

248

249

250

251

252

253

Unique effects of individual differences in performance levels on Cattell activation (BOLD) were found in regions similar to those activated by the main effect of the Cattell task (e.g. MDN), with the exception of the lateral occipital cortex and inclusion of inferior temporal gyrus, primary visual cortex, caudate and thalamus, (cf. Figure 2a and Figure 3 top panel). Unlike the case for main effects, task-negative regions (e.g., DMN) showed small to no significant associations with performance.

254

255

256

257

258

Unique effects of age were similar but weaker to the effect of age in the model without other predictors (cf. Figure 2b and Figure 3 middle panel). Unique positive associations between CBF and Cattell activation was observed in middle frontal gyrus and cuneus regions. Negative associations were observed in insular regions, posterior cingulate cortex, bilateral angular gyrus, precentral gyrus and superior frontal gyrus.

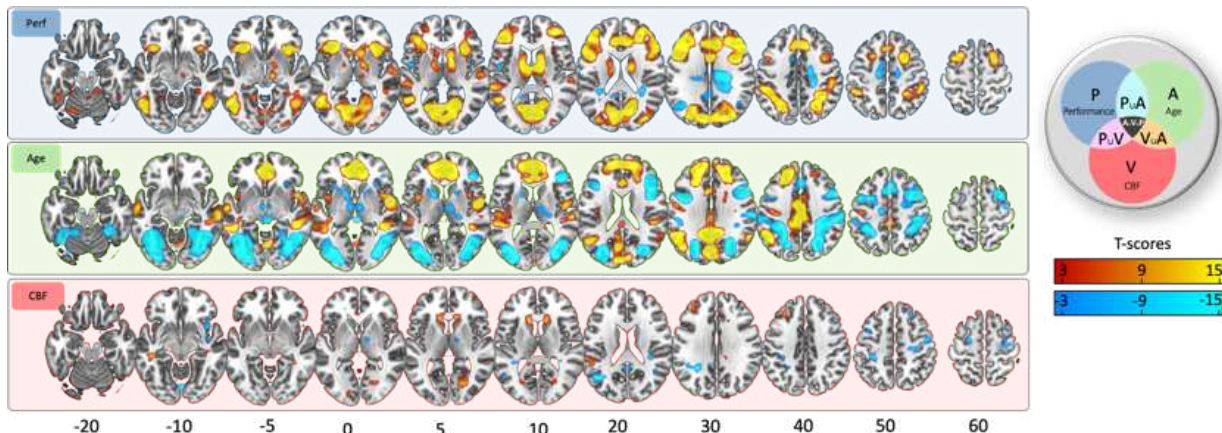
259

260

261

262

Unique effects of CBF were weak, but significant, showing positive associations with activation in the middle frontal gyrus, the putamen and the cuneus. Additionally, CBF was associated negatively with activation in task negative regions, namely the angular gyrus and precentral gyrus.



263
264
265
266
267

Figure 3. Unique effects in commonality analysis. (top panel) Age-related decreases (cold colours) and increases (warm colours). (middle panel) Performance-related decreases (cold colours) and increases (warm colours). (bottom panel) CBF-related decreases (cold colours) and increases (warm colours) in Cattell task. Slices are numbered by z level in Montreal Neurological Institute (MNI) space.

268

269 3.3.2. Common effects

270 There were many common effects between age and performance, with a positive
271 commonality coefficient ($C_{Age,P}$, Figure 4, cyan colour), i.e. a portion of the age effects on Cattell
272 activation was related to performance effects on Cattell activation. These effects were observed
273 in task positive (e.g. MDN) and task negative regions (e.g. DMN), in addition to thalamus, caudate,
274 primary motor cortex.

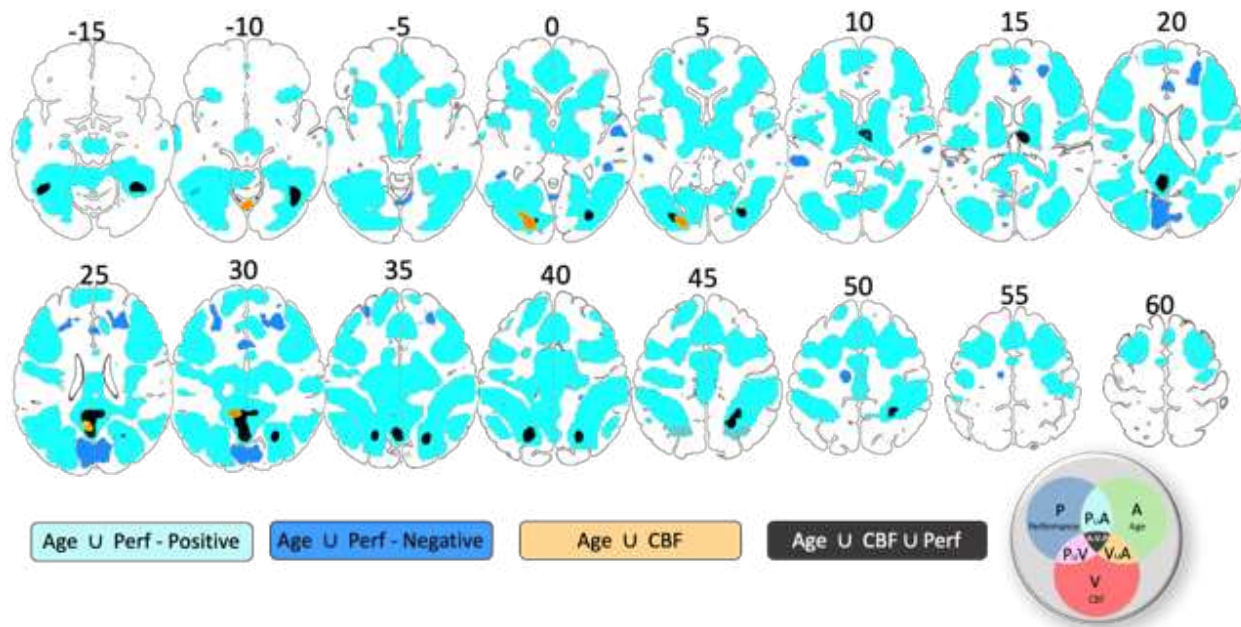
275 Negative commonality coefficients between performance and age were observed in the
276 cuneus, bilateral middle frontal gyrus, anterior and middle cingulate gyrus, and bilateral superior
277 temporal gyrus (dark blue colour in Figure 4). Negative values of commonality coefficients
278 indicate a suppressor relationship between predictors (Zientek and Thompson, 2006), i.e. the
279 effects of age and/or performance are stronger with their joint consideration in the model.

280 Confounding effects of baseline CBF on Cattell activation were characterised by the
281 common effect between Age and CBF ($C_{CBF,Age}$). Significant confounding effects were localised
282 within posterior cingulate cortex, fusiform gyrus and inferior occipital gyrus (orange colour in
283 Figure 4).

284 Performance-related effects of baseline CBF on Cattell activation were characterised by
285 the common effect between Age, CBF and Performance ($C_{CBF,Age,P}$, black colour in Figure 4).
286 Regions included intraparietal sulcus, posterior cingulate cortex, precuneus, thalamus and
287 fusiform gyrus. Furthermore, consistent with previous findings (Tsvetanov et al., 2018),
288 behaviourally-relevant effects were seen in inferior temporal and adjacent occipital regions,
289 presumably due to attentional enhancement of visual representations in the more difficult
290 conditions (Fedorenko et al., 2013).

291

292



293
294
295
296
297

Figure 4. Common Effects in commonality analysis. Positive and negative common effects between age and performance are shown in cyan and dark blue colours, respectively. Common effects between age and baseline CBF are shown in orange colour. Common effects between age, performance and CBF are shown in black colour. P – performance, A – age, V – vascular, i.e. CBF. Slices are numbered by z level in Montreal Neurological Institute (MNI) space.

298

299 4. Discussion

300 The study confirmed the prediction that regional cerebral blood flow (CBF) can explain
301 both performance-related and age-dependent components of the fMRI BOLD signal in parts of
302 the multiple-demand network (MDN) associated with more complex reasoning during a common
303 test of fluid intelligence (Cattell task). The age-dependent differences in baseline CBF also
304 explained variance in fMRI BOLD signal in some regions that was not related to task-performance.
305 We propose that modelling the effects of age on baseline CBF, and in general cerebrovascular
306 and neurovascular health (Tsvetanov et al., 2021), improves the interpretation of fMRI studies,
307 with implications for understanding brain health with ageing and disease, and that maintaining
308 brain perfusion as we get older may have a protective effect on brain function and cognition.
309

310 4.1. Age differences in baseline cerebral blood flow are related to behaviour-relevant 311 Cattell BOLD activity

312 Age-related decreases in baseline cerebral blood flow (CBF), assessed with a non-invasive
313 MR-perfusion technique, related to behaviourally relevant BOLD activity evoked by demanding
314 problem-solving. Our findings are consistent with previous studies relating baseline CBF to
315 performance on tasks carried outside the scanner (Bangen et al., 2014; Hays et al., 2017). We
316 extend these lines of work by showing that baseline CBF is linked to BOLD activity, with
317 behavioural correlation across individuals. Age-related decrease in CBF and decline in
318 performance related to a lower range of activation in task-positive regions and less deactivation

319 of task-negative regions. Of all task-positive regions, the bilateral intra-parietal sulcus, the
320 thalamus, and the fusiform gyrus showed significant common effects between age, CBF and
321 performance. The intraparietal sulcus and the thalamus also showed a unique association
322 between performance and BOLD activity, suggesting a neural origin of the effects in these
323 regions. The processes contributing to coupling between baseline CBF and neural activity are
324 multifaceted, probably comprising neurogenic vasodilation, cardiac output and arterial
325 remodelling (Gaballa et al., 1998; Ohanian et al., 2014; Li et al., 2015), all of which change with
326 age and regulate baseline and stimulus-evoked CBF (Willie et al., 2014). Establishing the relative
327 contribution and importance of these processes warrants future research.

328 Of all task-negative regions, only the posterior cingulate cortex showed common effects
329 between age, CBF and performance in predicting BOLD activation in the Cattell task. In this
330 region, age-related reduction in CBF and performance correlated with less deactivation in the
331 posterior cingulate cortex. The posterior cingulate cortex did not show unique effects between
332 performance and BOLD activity, suggesting a mechanism different from the one observed in task-
333 positive regions, likely reflecting a non-neuronal origin of the effects (see also “Unique effects of
334 performance, age and CBF in Cattell task”). While the deactivation of the default network in
335 young adults is thought to reflect suppression of neuronal activity (Fox et al., 2018), in the present
336 study, some of the poor performing older adults showed an over-activation, not less deactivation.
337 This again suggests a different involvement of the posterior cingulate cortex in older adults
338 compared to young adults, for instance, signals of non-neuronal origin caused by physiological
339 artifacts (Birn et al., 2006; Tsvetanov et al., 2021) or ‘vascular steal’ (Shmuel et al., 2002). Taken
340 together, these findings may reflect compromised vasodilatory reserve, resulting in an inefficient
341 redirection of resources from task-positive regions to task-negative regions in the attempt to
342 meet higher energy demands in task-positive regions, perhaps reflecting blood flow-dependent
343 glycolysis and oxidative metabolism. The breath of these associations is consistent with theories
344 of vasoactive and cardiovascular regulation of cerebral blood flow (Sobczyk et al., 2014; Digernes
345 et al., 2017).

346

347 4.2. Vascular Confounding effects of CBF on task-related activity

348 Only a portion of the age differences in performance-independent BOLD activation were
349 associated CBF decreases. Furthermore, the effects were observed in non-classical demand
350 network task-positive and task-negative regions not showing unique associations between
351 performance and BOLD activity, namely the fusiform gyrus and the posterior cingulate cortex
352 (Figure 4, orange regions). This is consistent with the view that differences in baseline CBF can
353 affect the sign and the magnitude of the evoked BOLD signal, without affecting changes in the
354 underlying neural activity (Cohen et al., 2002; Brown et al., 2003; Stefanovic et al., 2006). We
355 extend prior findings by showing that only a portion of the CBF effects can introduce such a
356 behaviourally irrelevant bias; other parts of the CBF variance might be related to behaviour-
357 relevant signal, i.e. differences in CBF could be important in their own right. Unlike the
358 normalisation approach described in Introduction to control for CBF differences, the current
359 commonality framework allows partition of CBF effects into effects of interest and effects of no
360 interest. We propose that modelling the effects of age on baseline CBF, and in general
361 cerebrovascular and neurovascular health (Tsvetanov et al., 2021), has implications for the
362 interpretation of fMRI studies of ageing, whereby it can improve brain-behaviour relationships

363 and provide a viable mechanistic account of maintaining and improving cognitive function in old
364 age.

365

366 4.3. Unique effects of performance, age and CBF on task-related activity

367

368 After accounting for age and performance, higher baseline cerebral blood flow remained
369 significantly associated with the level of BOLD activity in cortical regions modulated by
370 demanding problem-solving processes (Figure 3). Higher baseline CBF related to higher range of
371 activation in task positive regions under more demanding processing, including the middle frontal
372 gyrus, the putamen, and the cuneus. The effects were spatially adjacent or overlapping with
373 behaviour-relevant region suggesting that higher baseline CBF may provide the conditions to
374 upregulate activity in these regions, possibly through functional hyperaemia. Additionally, higher
375 CBF provided higher range of deactivation in task negative regions, namely the angular gyrus and
376 precentral gyrus. These effects were spatially adjacent or overlapping with regions showing
377 inefficient deactivation with ageing and suggest that higher baseline CBF may facilitate
378 suppression of activity in task-negative regions. This may reflect the effect of having an intact
379 vasodilatory reserve (Sobczyk et al., 2014; Digernes et al., 2017). Our findings have direct
380 implications for task-based BOLD imaging whereby higher baseline CBF levels contribute to
381 stronger changes in BOLD signal amplitude in response to demanding cognitive conditions. The
382 myogenic response and cardiac output are two major modulators of resting CBF (Hill et al., 2006;
383 Meng et al., 2015), which require future consideration to establish the mechanism underlying
384 our findings.

385 Ageing was associated with weaker activation of the multiple demand network and less
386 efficient suppression of the default network. These effects were over and above performance
387 and CBF, suggesting the involvement of additional factors leading to age-related difference in
388 BOLD activity. Some factors include genetics (Shan et al., 2016), cardiovascular and neurovascular
389 signals not captured by baseline CBF (Abdelkarim et al., 2019; Tsvetanov et al., 2021) or effects
390 of functional connectivity captured by regional activity (Tsvetanov et al., 2018). Age differences
391 in the shape of the haemodynamic response function (West et al., 2019) are less likely to
392 introduce bias in the current study given its block-related fMRI design (Liu et al., 2001). The
393 nature of these age effects should be elucidated through further investigation. The commonality
394 analysis framework provides a useful tool for multivariate simultaneous modelling to disentangle
395 the multifactorial nature of age-related BOLD differences.

396 After accounting for age, baseline CBF and other covariates of not interest, the level of
397 activity in the multiple-demand regions remained positively associated with performance during
398 the Cattell task in the scanner. Our findings are in line with previous studies during diverse
399 demanding tasks, including manipulations of working memory, target detection, response
400 inhibition (Fedorenko et al., 2013; Tschentscher et al., 2017; Assem et al., 2020a, 2020b). Given
401 that both age and cerebrovascular reactivity could introduce a very strong effect on the activity-
402 behaviour associations (even with narrow age range and healthy populations), our approach to
403 control for these factors, in combination with the population-based, large-sample, provide the
404 strongest evidence to date that individual differences variance in executive abilities is selectively
405 and robustly associated with the level of activity in the multiple demand network.

406 Our study adds evidence to the nature of suppression of the default network during
407 externally directed task (Buckner and DiNicola, 2019). The task-induced default network
408 deactivations were consistent with previous findings in the Cattell task (Samu et al., 2017) and in
409 general with the extent to which task conditions are cognitive demanding (Anticevic et al., 2012;
410 Sripada et al., 2020). The effects in the default network were related to age or baseline CBF, but
411 not uniquely related to performance, suggesting that the level of BOLD deactivations during
412 Cattell task do not reflect individual variability in cognitive performance. The nature of default
413 network suppression remains to be fully defined (Fox et al., 2018), but future findings about the
414 default network cannot be interpreted independent of age and baseline CBF, at least when
415 aiming to understand the relevance of DMN suppression in health and disease.
416

417 5. Issues and future directions

418
419 There are issues to the study. Our findings are based on a population-based cross-
420 sectional cohort, which cannot directly speak to individual's progression over time (i.e, the ageing
421 process). We only assessed the brain activations/co-activations, but do not quantify brain
422 connectivity (Tsvetanov et al., 2016, 2020a; Geerligs et al., 2017; Samu et al., 2017; Bethlehem
423 et al., 2020), even though both may change with in cognitive ageing (Tsvetanov et al., 2018). The
424 relationship between baseline CBF and functional connectivity decouples with ageing (Galiano et
425 al., 2019), but the behavioural relevance of such decoupling remains unclear, albeit motivated by
426 prior work controlling for vascular effects from fMRI BOLD data (Tsvetanov et al., 2016; Geerligs
427 et al., 2017). Future work should also i) evaluate the effects of CBF under different cognitive
428 states (Campbell et al., 2015; Geerligs and Tsvetanov, 2016), ii) consider nonlinearities between
429 CBF and BOLD signal within individuals (Chen, 2019) and across the lifespan (Tsvetanov et al.,
430 2016; Tibon et al., 2021), and iii) the relevance of baseline CBF to stimulus-evoked CBF (Jennings
431 et al., 2005) and other measures of cerebrovascular reactivity in ageing (Tsvetanov et al., 2020b)
432 and neurodegenerative diseases (Chen, 2019).

433 6. Conclusion

434 We introduce a novel approach to neuroimaging that can dissociate between shared and
435 unique signals across multiple neuroimaging modalities. Using this method, we show the effects
436 of age on cerebral blood flow, task-related BOLD responses and performance. The results
437 demonstrate that cerebrovascular health (i.e., baseline cerebral blood flow) explains
438 confounding but also performance-related BOLD responses in fluid ability across the lifespan.
439 They highlight the importance of using resting CBF data to model, rather than simply normalise
440 for, differences in vascular health in task-based fMRI BOLD data (cf. Tsvetanov et al., 2021). Unlike
441 the normalisation approach, our approach allows simultaneous modelling of multiple measures
442 with independent contributions to cerebrovascular health. Here, we provide empirical evidence
443 in support of the mechanism underlying the link between baseline CBF and neurocognitive
444 function across the lifespan. The insights from our results may facilitate the development of new
445 strategies to maintain cognitive ability across the life span in health and disease.
446

447 7. Acknowledgements

448

449 This work is supported by the Guarantors of Brain (G101149), SCNU Study Abroad
450 Program for Elite Postgraduate Students, the Medical Research Council
451 (MC_UU_00005/12/SUAG004/051/RG91365; SUAG04/51 R101400) and the Cambridge NIHR
452 Biomedical Research Centre (BRC-1215-20014). The views expressed are those of the authors
453 and not necessarily those of the NIHR or the Department of Health and Social Care. For the
454 purpose of open access, the author has applied a CC BY public copyright licence to any Author
455 Accepted Manuscript version arising from this submission. The Cambridge Centre for Ageing and
456 Neuroscience (Cam-CAN) research was supported by the Biotechnology and Biological Sciences
457 Research Council (grant number BB/H008217/1). We thank the Cam-CAN respondents and their
458 primary care teams in Cambridge for their participation in this study. Further information about
459 the Cam-CAN corporate authorship membership can be found at

460 <https://www.cam-can.org/index.php?content=corpauth#13>.

461

462 8. Competing Interests statement

463

464 J.B.R. serves as an associate editor to Brain and is a non- remunerated trustee of the
465 Guarantors of Brain, Darwin College Cambridge, and the PSP Association (UK). He has provided
466 consultancy to Asceneuron, Biogen, UCB and has research grants from AZ-Medimmune, Janssen,
467 Lilly and WAVE as industry partners in the Dementias Platform UK. The other authors have no
468 disclosures.

469

470 9. References

471 Abdelkarim D, Zhao Y, Turner MP, Sivakolundu DK, Lu H, Rypma B (2019) A neural-vascular
472 complex of age-related changes in the human brain: Anatomy, physiology, and implications
473 for neurocognitive aging. *Neurosci Biobehav Rev* 107:927–944 Available at:
474 <http://www.ncbi.nlm.nih.gov/pubmed/31499083> [Accessed September 26, 2019].

475 Addicott MA, Yang LL, Peiffer AM, Burnett LR, Burdette JH, Chen MY, Hayasaka S, Kraft RA,
476 Maldjian JA, Laurienti PJ (2009) The effect of daily caffeine use on cerebral blood flow: How
477 much caffeine can we tolerate? *Hum Brain Mapp* 30:3102–3114.

478 Anticevic A, Cole MW, Murray JD, Corlett PR, Wang X-J, Krystal JH (2012) The role of default
479 network deactivation in cognition and disease. *Trends Cogn Sci* 16:584–592 Available at:
480 <http://www.ncbi.nlm.nih.gov/pubmed/23142417> [Accessed August 2, 2013].

481 Assem M, Blank IA, Mineroff Z, Ademoğlu A, Fedorenko E (2020a) Activity in the fronto-parietal
482 multiple-demand network is robustly associated with individual differences in working
483 memory and fluid intelligence. *Cortex* 131:1–16.

484 Assem M, Glasser MF, Van Essen DC, Duncan J (2020b) A Domain-General Cognitive Core Defined
485 in Multimodally Parcellated Human Cortex. *Cereb Cortex* 30:4361–4380 Available at:
486 <https://academic.oup.com/cercor/article/30/8/4361/5815289> [Accessed June 28, 2021].

487 Bangen KJ, Nation DA, Clark LR, Harmell AL, Wierenga CE, Dev SI, Delano-Wood L, Zlatar ZZ,

488 Salmon DP, Liu TT, Bondi MW (2014) Interactive effects of vascular risk burden and advanced
489 age on cerebral blood flow. *Front Aging Neurosci* 6:1–10.

490 Bethlehem RAI, Paquola C, Seidlitz J, Ronan L, Bernhardt B, Consortium C-C, Tsvetanov KA (2020)
491 Dispersion of functional gradients across the adult lifespan. *Neuroimage*:117299 Available
492 at: <https://linkinghub.elsevier.com/retrieve/pii/S1053811920307850> [Accessed August 27,
493 2020].

494 Birn RM, Diamond JB, Smith M a, Bandettini P a (2006) Separating respiratory-variation-related
495 fluctuations from neuronal-activity-related fluctuations in fMRI. *Neuroimage* 31:1536–1548
496 Available at: <http://www.ncbi.nlm.nih.gov/pubmed/16632379> [Accessed February 28,
497 2013].

498 Brown GG, Eyler Zorrilla LT, Georgy B, Kindermann SS, Wong EC, Buxton RB (2003) BOLD and
499 perfusion response to finger-thumb apposition after acetazolamide administration:
500 differential relationship to global perfusion. *J Cereb Blood Flow Metab* 23:829–837 Available
501 at: <http://www.ncbi.nlm.nih.gov/pubmed/12843786> [Accessed October 1, 2019].

502 Buckner RL, Andrews-Hanna JR, Schacter DL (2008) The brain's default network: anatomy,
503 function, and relevance to disease. *Ann N Y Acad Sci* 1124:1–38 Available at:
504 <http://www.ncbi.nlm.nih.gov/pubmed/18400922> [Accessed May 21, 2013].

505 Buckner RL, DiNicola LM (2019) The brain's default network: updated anatomy, physiology and
506 evolving insights. *Nat Rev Neurosci* 20:593–608 Available at: www.nature.com/nrn
507 [Accessed June 29, 2021].

508 Cabeza R, Albert M, Belleville S, Craik FIM, Duarte A, Grady CL, Lindenberger U, Nyberg L, Park
509 DC, Reuter-Lorenz PA, Rugg MD, Steffener J, Rajah MN (2018) Maintenance, reserve and
510 compensation: the cognitive neuroscience of healthy ageing. *Nat Rev Neurosci* 19:701–710
511 Available at: <http://www.nature.com/articles/s41583-018-0068-2> [Accessed March 3,
512 2019].

513 Camilleri JA, Müller VI, Fox P, Laird AR, Hoffstaedter F, Kalenscher T, Eickhoff SB (2018) Definition
514 and characterization of an extended multiple-demand network. *Neuroimage* 165:138–147
515 Available at: <https://pubmed.ncbi.nlm.nih.gov/29030105/> [Accessed December 15, 2020].

516 Campbell KL et al. (2015) Idiosyncratic responding during movie-watching predicted by age
517 differences in attentional control. *Neurobiol Aging* 36:3045–3055.

518 Cattell RB (1971) Abilities: Their structure growth and action. Boston, MA: Houghton Mifflin.

519 Chen JJ (2019) Functional MRI of brain physiology in aging and neurodegenerative diseases.
520 *Neuroimage* 187:209–225.

521 Chen JJ, Rosas HD, Salat DH (2011) Age-associated reductions in cerebral blood flow are
522 independent from regional atrophy. *Neuroimage* 55:468–478 Available at:
523 <http://www.sciencedirect.com/science/article/pii/S1053811910016162> [Accessed March
524 21, 2014].

525 Cohen ER, Ugurbil K, Kim S-G (2002) Effect of Basal Conditions on the Magnitude and Dynamics
526 of the Blood Oxygenation Level-Dependent fMRI Response. *J Cereb Blood Flow Metab*
527 22:1042–1053 Available at: <http://www.ncbi.nlm.nih.gov/pubmed/12218410> [Accessed
528 September 29, 2019].

529 Crittenden BM, Mitchell DJ, Duncan J (2016) Task encoding across the multiple demand cortex is
530 consistent with a frontoparietal and cingulo-opercular dual networks distinction. *J Neurosci*
531 36:6147–6155 Available at: <https://www.jneurosci.org/content/36/23/6147> [Accessed

532 December 15, 2020].

533 Digernes I, Bjørnerud A, Vatnehol SAS, Løvland G, Courivaud F, Vik-Mo E, Meling TR, Emblem KE
 534 (2017) A theoretical framework for determining cerebral vascular function and
 535 heterogeneity from dynamic susceptibility contrast MRI: J Cereb Blood Flow Metab
 536 37:2237–2248 Available at:
 537 <https://journals.sagepub.com/doi/full/10.1177/0271678X17694187> [Accessed August 13,
 538 2021].

539 Domino EF, Ni L, Xu Y, Koepp RA, Guthrie S, Zubieta JK (2004) Regional cerebral blood flow and
 540 plasma nicotine after smoking tobacco cigarettes. Prog Neuro-Psychopharmacology Biol
 541 Psychiatry 28:319–327.

542 Duncan J (2010) The multiple-demand (MD) system of the primate brain: mental programs for
 543 intelligent behaviour. Trends Cogn Sci 14:172–179 Available at:
 544 <http://www.ncbi.nlm.nih.gov/pubmed/20171926> [Accessed October 17, 2013].

545 Duncan J (2013) The structure of cognition: attentional episodes in mind and brain. Neuron
 546 80:35–50.

547 Fedorenko E, Duncan J, Kanwisher N (2013) Broad domain generality in focal regions of frontal
 548 and parietal cortex. Proc Natl Acad Sci U S A 110:16616–16621 Available at:
 549 <https://pubmed.ncbi.nlm.nih.gov/24062451/> [Accessed May 19, 2021].

550 Folstein MF, Folstein SE, McHugh PR (1975) “Mini-mental state.” J Psychiatr Res 12:189–198
 551 Available at: <http://www.sciencedirect.com/science/article/pii/0022395675900266>
 552 [Accessed February 21, 2014].

553 Fox K, Foster B, Kucyi A, Daitch A, Parvizi J (2018) Intracranial Electrophysiology of the Human
 554 Default Network. Trends Cogn Sci 22:307–324 Available at:
 555 <https://pubmed.ncbi.nlm.nih.gov/29525387/> [Accessed August 20, 2021].

556 Friston KJ, Ashburner J, Kiebel S, Nichols T, Penny WD (2007) Statistical parametric mapping : the
 557 analysis of functional brain images. Elsevier Academic Press.

558 Gaballa MA, Jacob CT, Raya TE, Liu J, Simon B, Goldman S (1998) Large Artery Remodeling During
 559 Aging. Hypertension 32:437–443 Available at:
 560 <https://www.ahajournals.org/doi/abs/10.1161/01.HYP.32.3.437> [Accessed August 20,
 561 2021].

562 Galiano A, Mengual E, García de Eulate R, Galdeano I, Vidorreta M, Recio M, Riverol M, Zubieta
 563 JL, Fernández-Seara MA (2019) Coupling of cerebral blood flow and functional connectivity
 564 is decreased in healthy aging. Brain Imaging Behav:1–15 Available at:
 565 <http://link.springer.com/10.1007/s11682-019-00157-w> [Accessed September 26, 2019].

566 Geerligs L, Tsvetanov KA (2016) The use of resting state data in an integrative approach to
 567 studying neurocognitive ageing – Commentary on Campbell and Schacter (2016). Lang Cogn
 568 Neurosci 32:684–691.

569 Geerligs L, Tsvetanov KA, Cam-Can, Henson RN (2017) Challenges in measuring individual
 570 differences in functional connectivity using fMRI: The case of healthy aging. Hum Brain
 571 Mapp.

572 Grade M, Hernandez Tamames JA, Pizzini FB, Achten E, Golay X, Smits M (2015) A
 573 neuroradiologist’s guide to arterial spin labeling MRI in clinical practice. Neuroradiology
 574 57:1181–1202.

575 Hays CC, Zlatar ZZ, Campbell L, Meloy MJ, Wierenga CE (2017) Temporal gradient during famous

576 face naming is associated with lower cerebral blood flow and gray matter volume in aging.
577 *Neuropsychologia* 107:76–83 Available at: <https://pubmed.ncbi.nlm.nih.gov/29133109/>
578 [Accessed July 11, 2020].

579 Henriksen OM, Vestergaard MB, Lindberg U, Aachmann-Andersen NJ, Lisbjerg K, Christensen SJ,
580 Rasmussen P, Olsen N V., Forman JL, Larsson HBW, Law I (2018) Interindividual and regional
581 relationship between cerebral blood flow and glucose metabolism in the resting brain.
582 <https://doi.org/101152/japplphysiol002762018> 125:1080–1089 Available at:
583 <https://journals.physiology.org/doi/abs/10.1152/japplphysiol.00276.2018> [Accessed
584 September 22, 2021].

585 Hill MA, Davis MJ, Meininger GA, Potocnik SJ, Murphy T V. (2006) Arteriolar myogenic signalling
586 mechanisms: Implications for local vascular function. *Clin Hemorheol Microcirc* 34:67–79.

587 Horn JL, Cattell RB (1967) Age differences in fluid and crystallized intelligence. *Acta Psychol*
588 (Amst) 26:107–129.

589 Hutchison JL, Lu H, Rypma B (2013) Neural Mechanisms of Age-Related Slowing: The
590 Δ CBF/ Δ CMRO₂ Ratio Mediates Age-Differences in BOLD Signal and Human Performance.
591 *Cereb cortex* 23:2337–2346 Available at: <http://www.ncbi.nlm.nih.gov/pubmed/22879349>
592 [Accessed November 27, 2012].

593 Iadecola C (2004) Neurovascular regulation in the normal brain and in Alzheimer's disease. *Nat*
594 *Rev Neurosci* 5:347–360 Available at: <http://www.nature.com/doifinder/10.1038/nrn1387>
595 [Accessed August 15, 2017].

596 Jennings JR, Muldoon MF, Ryan C, Price JC, Greer P, Sutton-Tyrrell K, Veen FM van der, Meltzer
597 CC (2005) Reduced cerebral blood flow response and compensation among patients with
598 untreated hypertension. *Neurology* 64:1358–1365 Available at:
599 <https://n.neurology.org/content/64/8/1358> [Accessed August 21, 2021].

600 Kaufman AS, Horn JL (1996) Age changes on tests of fluid and crystallized ability for women and
601 men on the Kaufman Adolescent and Adult Intelligence Test (KAIT) at ages 17-94 years. *Arch*
602 *Clin Neuropsychol* 11:97–121.

603 Kennedy KM, Raz N (2015) Normal Aging of the Brain. In: *Brain Mapping*, pp 603–617. Elsevier.
604 Available at: <https://linkinghub.elsevier.com/retrieve/pii/B9780123970251000683>
605 [Accessed February 5, 2019].

606 Kievit RA et al. (2014) Distinct aspects of frontal lobe structure mediate age-related differences
607 in fluid intelligence and multitasking. *Nat Commun* 5:5658 Available at:
608 <http://www.nature.com/doifinder/10.1038/ncomms6658> [Accessed September 13, 2017].

609 Kisler K, Nelson AR, Montagne A, Zlokovic B V. (2017) Cerebral blood flow regulation and
610 neurovascular dysfunction in Alzheimer disease. *Nat Rev Neurosci* 18:419–434 Available at:
611 <http://www.ncbi.nlm.nih.gov/pubmed/28515434> [Accessed August 18, 2017].

612 Kraha A, Turner H, Nimon K, Zientek LR, Henson RK (2012) Tools to Support Interpreting Multiple
613 Regression in the Face of Multicollinearity. *Front Psychol* 3:44 Available at:
614 <http://journal.frontiersin.org/article/10.3389/fpsyg.2012.00044/abstract> [Accessed August
615 22, 2017].

616 Leeuwis AE, Smith LA, Melbourne A, Hughes AD, Richards M, Prins ND, Sokolska M, Atkinson D,
617 Tillin T, Jäger HR, Chaturvedi N, Flier WM van der, Barkhof F (2018) Cerebral Blood Flow and
618 Cognitive Functioning in a Community-Based, Multi-Ethnic Cohort: The SABRE Study. *Front*
619 *Aging Neurosci* 10:279 Available at:

620 <https://www.frontiersin.org/article/10.3389/fnagi.2018.00279/full> [Accessed December 17, 2020].

621 Lemkuil BP, Drummond JC, Patel PM (2013) Central Nervous System Physiology: Cerebrovascular. Pharmacol Physiol Anesth Found Clin Appl:123–136.

622 Li Y, Shen Q, Huang S, Li W, Muir E, Long J, TQ D (2015) Cerebral angiography, blood flow and vascular reactivity in progressive hypertension. Neuroimage 111:329–337 Available at: <https://pubmed.ncbi.nlm.nih.gov/25731987/> [Accessed August 20, 2021].

623 Liu P, Hebrank AC, Rodrigue KM, Kennedy KM, Section J, Park DC, Lu H (2013) Age-related differences in memory-encoding fMRI responses after accounting for decline in vascular reactivity. Neuroimage 78:415–425 Available at: <http://www.ncbi.nlm.nih.gov/pubmed/23624491> [Accessed October 24, 2013].

624 Liu TT, Frank LR, Wong EC, Buxton RB (2001) Detection Power, Estimation Efficiency, and Predictability in Event-Related fMRI. Neuroimage 13:759–773.

625 Meng L, Hou W, Chui J, Han R, Gelb A (2015) Cardiac Output and Cerebral Blood Flow: The Integrated Regulation of Brain Perfusion in Adult Humans. Anesthesiology 123:1198–1208 Available at: <https://pubmed.ncbi.nlm.nih.gov/26402848/> [Accessed August 13, 2021].

626 Merola A, Germuska MA, Warnert EA, Richmond L, Helme D, Khot S, Murphy K, Rogers PJ, Hall JE, Wise RG (2017) Mapping the pharmacological modulation of brain oxygen metabolism: The effects of caffeine on absolute CMRO₂ measured using dual calibrated fMRI. Neuroimage 155:331–343 Available at: <https://www.sciencedirect.com/science/article/pii/S1053811917302367?via%3Dihub> [Accessed October 7, 2019].

627 Mishra A, Hall CN, Howarth C, Freeman RD (2021) Key relationships between non-invasive functional neuroimaging and the underlying neuronal activity. Philos Trans R Soc B Biol Sci 376:20190622 Available at: <https://royalsocietypublishing.org/doi/10.1098/rstb.2019.0622> [Accessed December 17, 2020].

628 Mutsaerts HJ, Petr J, Václavů L, van Dalen JW, Robertson AD, Caan MW, Masellis M, Nederveen AJ, Richard E, MacIntosh BJ (2017) The spatial coefficient of variation in arterial spin labeling cerebral blood flow images. J Cereb Blood Flow Metab 37:3184–3192 Available at: <http://www.ncbi.nlm.nih.gov/pubmed/28058975> [Accessed June 25, 2019].

629 Mutsaerts HJMM et al. (2018) Comparison of arterial spin labeling registration strategies in the multi-center GENetic frontotemporal dementia initiative (GENFI). J Magn Reson Imaging 47:131–140 Available at: <http://www.ncbi.nlm.nih.gov/pubmed/28480617> [Accessed September 16, 2019].

630 Nimon K, Lewis M, Kane R, Haynes RM (2008) An R package to compute commonality coefficients in the multiple regression case: An introduction to the package and a practical example. Behav Res Methods 40:457–466.

631 Ohanian J, Liao A, Forman SP, Ohanian V (2014) Age-related remodeling of small arteries is accompanied by increased sphingomyelinase activity and accumulation of long-chain ceramides. Physiol Rep 2 Available at: [/pmc/articles/PMC4098743/](https://pmc/articles/PMC4098743/) [Accessed August 20, 2021].

632 Patricia C, Henk-Jan M, Eidrees G, Marion S, Marjan A, Egill R, Francesca Benedetta P, Jorge J, Mervi K, Ritva V, António B-L, Roland W, Elna-Marie L, Eric A (2014) Review of confounding effects on perfusion measurements. Front Hum Neurosci 8 Available at: <https://www.ncbi.nlm.nih.gov/pmc/articles/PMC4098743/> [Accessed August 20, 2021].

664 http://www.frontiersin.org/Community/AbstractDetails.aspx?ABS_DOI=10.3389/conf.fnhu
665 m.2014.214.00073 [Accessed October 4, 2019].

666 Piguet O, Hornberger M, Shelley BP, Kipps CM, Hodges JR (2009) Sensitivity of current criteria for
667 the diagnosis of behavioral variant frontotemporal dementia. *Neurology* 72:732–737.

668 Raichle ME (2015) The Brain’s Default Mode Network. *Annu Rev Neurosci*:413–427.

669 Rorden C, Brett M (2000) Stereotaxic display of brain lesions. *Behav Neurol* 12:191–200 Available
670 at: <https://pubmed.ncbi.nlm.nih.gov/11568431/> [Accessed November 8, 2021].

671 Salthouse T (2012) Consequences of age-related cognitive declines. *Annu Rev Psychol* 63:201–
672 226 Available at: <http://www.ncbi.nlm.nih.gov/pubmed/21740223> [Accessed November
673 27, 2012].

674 Salthouse TA, Atkinson TM, Berish DE (2003) Executive functioning as a potential mediator of
675 age-related cognitive decline in normal adults. *J Exp Psychol Gen* 132:566–594.

676 Samu D et al. (2017) Preserved cognitive functions with age are determined by domain-
677 dependent shifts in network responsivity. *Nat Commun* 8:ncomms14743.

678 Shafto MA et al. (2014) The Cambridge Centre for Ageing and Neuroscience (Cam-CAN) study
679 protocol: A cross-sectional, lifespan, multidisciplinary examination of healthy cognitive
680 ageing. *BMC Neurol* 14.

681 Shan ZY, Vinkhuyzen AAE, Thompson PM, McMahon KL, Blokland GAM, de Zubiray GI, Calhoun
682 V, Martin NG, Visscher PM, Wright MJ, Reutens DC (2016) Genes influence the amplitude
683 and timing of brain hemodynamic responses. *Neuroimage* 124:663–671.

684 Shmuel A, Yacoub E, Pfeuffer J, Van de Moortele PF, Adriany G, Hu X, Ugurbil K (2002) Sustained
685 negative BOLD, blood flow and oxygen consumption response and its coupling to the
686 positive response in the human brain. *Neuron* 36:1195–1210.

687 Skinner HA (1982) The drug abuse screening test. *Addict Behav* 7:363–371.

688 Smith SM, Nichols TE (2009) Threshold-free cluster enhancement: Addressing problems of
689 smoothing, threshold dependence and localisation in cluster inference. *Neuroimage* 44:83–
690 98 Available at: <https://pubmed.ncbi.nlm.nih.gov/18501637/> [Accessed June 21, 2021].

691 Snellen H (1862) *Probekbuchstaben zur bestimmung der sehscharfe*. Utrecht: Van de Weijer.

692 Sobczyk O, Battisti-Charbonney a, Fierstra J, Mandell DM, Poublanc J, Crawley a P, Mikulis DJ,
693 Duffin J, Fisher J a (2014) A conceptual model for CO₂-induced redistribution of cerebral
694 blood flow with experimental confirmation using BOLD MRI. *Neuroimage* 92C:56–68
695 Available at: <http://www.ncbi.nlm.nih.gov/pubmed/24508647> [Accessed March 22, 2014].

696 Sripada C, Angstadt M, Rutherford S, Taxali A, Shadden K (2020) Toward a “treadmill test” for
697 cognition: Improved prediction of general cognitive ability from the task activated brain.
698 *Hum Brain Mapp* 41:3186–3197 Available at:
699 <https://onlinelibrary.wiley.com/doi/full/10.1002/hbm.25007> [Accessed June 28, 2021].

700 Stefanovic B, Warnking JM, Rylander KM, Pike GB (2006) The effect of global cerebral vasodilation
701 on focal activation hemodynamics. *Neuroimage* 30:726–734.

702 Sweeney MD, Kisler K, Montagne A, Toga AW, Zlokovic B V. (2018) The role of brain vasculature
703 in neurodegenerative disorders. *Nat Neurosci* 21:1318–1331.

704 Sweeney MD, Zhao Z, Montagne A, Nelson AR, Zlokovic B V. (2019) Blood-brain barrier: From
705 physiology to disease and back. *Physiol Rev* 99:21–78.

706 Taylor JR, Williams N, Cusack R, Auer T, Shafto MA, Dixon M, Tyler LK, Cam-Can, Henson RN (2015)
707 The Cambridge Centre for Ageing and Neuroscience (Cam-CAN) data repository: Structural

708 and functional MRI, MEG, and cognitive data from a cross-sectional adult lifespan sample.
709 *Neuroimage* Available at:
710 <http://www.sciencedirect.com/science/article/pii/S1053811915008150> [Accessed
711 September 21, 2015].

712 Tibon R, Tsvetanov KA, Price D, Nesbitt D, CAN C, Henson R (2021) Transient neural network
713 dynamics in cognitive ageing. *Neurobiol Aging* 105:217–228.

714 Tschentscher N, Mitchell D, Duncan J (2017) Fluid intelligence predicts novel rule implementation
715 in a distributed frontoparietal control network. *J Neurosci* 37:4841–4847.

716 Tsvetanov KA et al. (2020a) Brain functional network integrity sustains cognitive function despite
717 atrophy in presymptomatic genetic frontotemporal dementia. *Alzheimer's
718 Dement:alz.12209* Available at: <https://onlinelibrary.wiley.com/doi/10.1002/alz.12209>
719 [Accessed December 9, 2020].

720 Tsvetanov KA, Henson RNA, Jones PS, Mutsaerts H, Fuhrmann D, Tyler LK, Rowe JB (2020b) The
721 effects of age on resting-state BOLD signal variability is explained by cardiovascular and
722 cerebrovascular factors. In: *Psychophysiology*. Blackwell Publishing Inc. Available at:
723 <https://onlinelibrary.wiley.com/doi/full/10.1111/psyp.13714> [Accessed December 9,
724 2020].

725 Tsvetanov KA, Henson RNA, Rowe JB (2021) Separating vascular and neuronal effects of age on
726 fMRI BOLD signals. *Philos Trans R Soc London Ser B, Biol Sci* 376:20190631.

727 Tsvetanov KA, Henson RNA, Tyler LK, Davis SW, Shafto MA, Taylor JR, Williams N, Rowe JB (2015)
728 The effect of ageing on fMRI: Correction for the confounding effects of vascular reactivity
729 evaluated by joint fMRI and MEG in 335 adults. *Hum Brain Mapp* 36:2248–2269 Available
730 at: <http://www.ncbi.nlm.nih.gov/pubmed/25727740> [Accessed February 27, 2015].

731 Tsvetanov KA, Henson RNA, Tyler LK, Razi A, Geerligs L, Ham TE, Rowe JB (2016) Extrinsic and
732 intrinsic brain network connectivity maintains cognition across the lifespan despite
733 accelerated decay of regional brain activation. *J Neurosci* 36:3115–3126.

734 Tsvetanov KA, Ye Z, Hughes L, Samu D, Treder MS, Wolpe N, Tyler LK, Rowe JB, for Cambridge
735 Centre for Ageing and Neuroscience (2018) Activity and connectivity differences underlying
736 inhibitory control across the adult lifespan. *J Neurosci* 38:7887–7900 Available at:
737 <http://www.ncbi.nlm.nih.gov/pubmed/30049889> [Accessed August 1, 2018].

738 United Nations D of E and SAPD (2020) World Population Ageing 2019.

739 West KL, Zuppichini MD, Turner MP, Sivakolundu DK, Zhao Y, Abdelkarim D, Spence JS, Rypma B
740 (2019) BOLD hemodynamic response function changes significantly with healthy aging.
741 *Neuroimage* 188:198–207.

742 Willie CK, Tzeng Y-C, Fisher JA, Ainslie PN (2014) Integrative regulation of human brain blood flow.
743 *J Physiol* 592:841–859 Available at: <http://www.ncbi.nlm.nih.gov/pubmed/24396059>
744 [Accessed October 1, 2019].

745 Woolgar A, Bor D, Duncan J (2013) Global increase in task-related fronto-parietal activity after
746 focal frontal lobe lesion. *J Cogn Neurosci* 25:1542–1552.

747 Woolgar A, Duncan J, Manes F, Fedorenko E (2018) Fluid intelligence is supported by the multiple-
748 demand system not the language system. *Nat Hum Behav* 2:200–204 Available at:
749 <https://pubmed.ncbi.nlm.nih.gov/31620646/> [Accessed December 15, 2020].

750 Yarchoan M, Xie SX, Kling MA, Toledo JB, Wolk DA, Lee EB, Van Deerlin V, Lee VMY, Trojanowski
751 JQ, Arnold SE (2012) Cerebrovascular atherosclerosis correlates with Alzheimer pathology

752 in neurodegenerative dementias. *Brain* 135:3749–3756.

753 Zhang N, Gordon ML, Ma Y, Chi B, Gomar JJ, Peng S, Kingsley PB, Eidelberg D, Goldberg TE (2018)
754 The Age-Related Perfusion Pattern Measured With Arterial Spin Labeling MRI in Healthy
755 Subjects. *Front Aging Neurosci* 10:214 Available at:
756 <http://www.ncbi.nlm.nih.gov/pubmed/30065646> [Accessed July 9, 2019].

757 Zientek LR, Thompson B (2006) Commonality analysis: Partitioning variance to facilitate better
758 understanding of data. *J Early Interv* 28:299–307 Available at:
759 <https://journals.sagepub.com/doi/abs/10.1177/105381510602800405?journalCode=jeib>
760 [Accessed June 21, 2021].

761 Zlokovic B V (2011) Neurovascular pathways to neurodegeneration in Alzheimer's disease and
762 other disorders. *Nat Rev Neurosci* 12:723–738 Available at:
763 <http://www.ncbi.nlm.nih.gov/pubmed/22048062> [Accessed August 19, 2017].

764

10. Figure Legends

1 Figure 1. Summary of the analytical pipeline.

2 Figure 2. Main and age effects on task-based activity and cerebral blood flow (CBF) maps.

3 (a) Main effects of BOLD activity in response to Hard vs Easy blocks with over- and
4 underactivations shown in warm and cold colours, respectively. (b) Age-related decreases (cold
5 colours) and increases (warm colours) in Cattell task. (c) Main effect of baseline CBF across all
6 participants. (d) Age-related decreases (cold colours) and increases (warm colours) in baseline
7 CBF. Slices are numbered by z level in Montreal Neurological Institute (MNI) space.

8
9 Figure 3. Unique effects in commonality analysis. (top panel) Age-related decreases (cold
10 colours) and increases (warm colours). (middle panel) Performance-related decreases (cold
11 colours) and increases (warm colours). (bottom panel) CBF-related decreases (cold colours) and
12 increases (warm colours) in Cattell task. Slices are numbered by z level in Montreal Neurological
13 Institute (MNI) space.

14
15 Figure 4. Common Effects in commonality analysis. Positive and negative common effects
16 between age and performance are shown in cyan and dark blue colours, respectively. Common
17 effects between age and baseline CBF are shown in orange colour. Common effects between age,
18 performance and CBF are shown in black colour. P – performance, A – age, V – vascular, i.e. CBF.
19 Slices are numbered by z level in Montreal Neurological Institute (MNI) space.

1

2 **11. Tables**

3

4 *Table 1. Participants' demographic information*

N=223		Decile						
		1	2	3	4	5	6	7
Age range [years]	Numbers	19-27	28-37	38-47	48-57	58-67	68-77	78-87
		21	39	37	35	35	30	26
Gender								
Male		9	19	18	17	18	16	14
Female		12	20	19	18	17	14	12
Handedness ^a								
Mean/SD		79/44	89/25	81/27	94/11	77/50	95/10	87/33
Range[min/max]		-100/100	-56/100	-56/100	58/100	-78/100	53/100	-56/100
Education ^b								
None		0	0	0	0	0	5	1
GCSE		2	2	6	3	3	3	3
A-level		4	1	3	11	9	8	9
University		15	36	28	21	23	14	13

5

6

7 ^a Higher scores indicate greater right-hand preference, as assessed by Edinburgh Handedness
8 Inventory (Oldfield, 1971).

9 ^b Categorized according to the British education system: "None" = no education over the age of 16
10 yrs; "GCSE" = General Certificate of Secondary Education; "A Levels" = General Certificate of Education
11 Advanced Level; "University" = undergraduate or graduate degree.

12

13

14